

This is the accepted manuscript made available via CHORUS. The article has been published as:

Modification of electronic structure in compressively strained vanadium dioxide films

T. J. Huffman, Peng Xu, A. J. Hollingshad, M. M. Qazilbash, Lei Wang, R. A. Lukaszew, S. Kittiwatanakul, J. Lu, and S. A. Wolf

Phys. Rev. B **91**, 205140 — Published 29 May 2015

DOI: [10.1103/PhysRevB.91.205140](https://doi.org/10.1103/PhysRevB.91.205140)

Modification of electronic structure in compressively strained vanadium dioxide films

T.J. Huffman¹, Peng Xu¹, A. J. Hollingshad¹, M. M. Qazilbash^{1,*}, Lei Wang¹, R.A. Lukaszew¹,
S. Kittiwatanakul², J. Lu², S. A. Wolf^{2,3}

¹*Department of Physics, College of William and Mary, Williamsburg, Virginia 23187-8795, USA*

²*Department of Material Sciences and Engineering, University of Virginia, Charlottesville, Virginia 22904, USA*

³*Department of Physics, University of Virginia, Charlottesville, Virginia 22904, USA*

Vanadium dioxide (VO₂) undergoes a phase transition between an insulating monoclinic (M₁) phase and a conducting rutile phase. Like other correlated electron systems, the properties of VO₂ can be extremely sensitive to small changes in external parameters such as strain. In this work, we investigate a compressively strained VO₂ film grown on [001] quartz substrate in which the phase transition temperature (T_c) has been depressed to 325K from the bulk value of 340K. Infrared and optical spectroscopy reveals that the lattice dynamics of this strained film are very similar to unstrained VO₂. However, some of the electronic inter-band transitions of the strained VO₂ film are significantly shifted in energy from those in unstrained VO₂. That the lattice dynamics remain largely unchanged, while the T_c and some of the electronic inter-band transitions differ substantially from the bulk values highlight the role of electronic correlations in driving this metal-insulator phase transition.

I. INTRODUCTION

Strongly interacting degrees of freedom in condensed matter systems often lead to novel emergent properties such as metal-insulator transitions, superconductivity, colossal magneto-resistance, and high-T_c superconductivity.¹⁻⁴ Because they arise from multiple strongly interacting degrees of freedom, these emergent properties are highly sensitive to external factors such as temperature, strain, chemical doping, and applied fields. The true potential of strongly correlated systems lies in this sensitivity to external parameters. With sufficient understanding, the properties of these materials could be *engineered* to match specific applications. The technological impact of harnessing these novel properties for applications cannot be overstated.

Additional experimental data is needed to further inform our understanding of these materials. Unfortunately, the same sensitivity to external parameters that makes these materials so promising for future applications also makes experimental characterization difficult. The emergent properties can vary widely between different samples of the same material, as different growth techniques and conditions result in variations in strain, stoichiometry, and microstructure. Thus, for experimental measurements of these systems to provide meaningful insight, the external parameters, the intrinsic interacting degrees of

freedom, and the resulting properties must all be well characterized. Hence, measurements on samples subject to external perturbations, for example pressure and strain^{5–10}, can provide additional insight into the underlying physics of these systems.

Vanadium dioxide (VO₂) is perhaps the canonical strongly correlated transition metal oxide; its relatively simple unit cell and stoichiometric composition make it an ideal material to study strong correlations. Bulk VO₂ undergoes a metal-insulator transition (MIT) at $T_c=340\text{K}$ between an insulating phase below T_c and a metallic phase above T_c . The MIT is accompanied by a structural transition between the insulating monoclinic M_1 lattice and the conducting rutile (tetragonal) lattice (See Fig. 1(a)). Despite extensive research, the precise relationship between the lattice structure and electronic properties remains elusive. As the vanadium atoms are in the 4+ valence state, there is expected to be one electron in the vanadium d -orbitals. The crystal field of the oxygen octahedron splits the vanadium d -orbitals into two higher energy e_g^σ orbitals, which contain lobes pointing towards the oxygen atoms, and the remaining three lower energy t_{2g} orbitals. The t_{2g} orbitals are additionally split into two e_g^π and one a_{1g} orbital. The a_{1g} band has lobes pointing along the rutile c_r (monoclinic M_1 a_M) axis and is slightly lower in energy than the e_g^π band.

Early on, a simple scheme was proposed by Goodenough to explain the role of the structural transition in the MIT in terms of the vanadium d -orbitals.¹¹ The structural change from rutile to monoclinic M_1 has two salient features: a dimerization of the vanadium atoms along the rutile c_r (a_M) direction, and an antiferroelectric type tilting of these vanadium dimers relative to the surrounding oxygen structure. Insulating behavior was proposed to arise as follows. The dimerization would lead to a splitting of the a_{1g} orbitals into bonding (a_{1g}) and anti-bonding (a_{1g}^*) bands, while the antiferroelectric tilting of the vanadium pairs would lead to an upshift of the e_g^π orbitals away from the Fermi energy to produce a gap between the filled bonding a_{1g} band and the empty e_g^π band¹¹. This effective band-structure scheme is qualitatively supported by experimental data on bulk crystals and thin films^{12–14}. However, a precise quantitative understanding of how this scheme is realized—in particular the roles of electronic correlations and the structural instability in the MIT—remains a matter of debate.^{15–18} A complete understanding of this correlated system is necessary to predict and control the emergent properties as a function of external parameters.

Broadband infrared and optical spectroscopy is a powerful technique for investigating the MIT in VO₂ because it provides insight into both the lattice and electronic structure, via the infrared active phonons and optical interband transitions, respectively. Previous infrared and optical spectroscopy experiments have been performed on bulk VO₂ and thin films.^{12–14,19,20} However, VO₂ films grown on different substrates and by different techniques can have significantly different strain states and microstructure. Because of the extreme sensitivity to external parameters in strongly correlated systems mentioned previously, accurate characterization of the strain and microstructure of various films, and the resultant emergent properties, can provide additional insight into the physics of these materials.

In this work we report the infrared and optical properties of a VO₂ film grown on a quartz substrate. The paper is organized as follows. We start with a thorough description of our preliminary characterization of the sample and then describe the infrared and optical spectroscopy experiments. Next, we report our results on the infrared active phonons in the M₁ phase. We then report and discuss the strain induced changes of the electronic inter-band transitions in both M₁ and rutile phases. We conclude with a brief summary of important results and their implications. Technical details of the experiment and data analysis, as well as tabulated optical constants of the VO₂ film, are presented in the Supplemental Material.²¹

II. EXPERIMENTAL METHODS

A. Sample characterization

The VO₂ film used in this experiment is a 70nm thick VO₂ film on a 0.5 mm thick (001) quartz substrate. The film was synthesized using the Reactive Biased Target Ion Beam Deposition (RBTIBD) method.²² The growth conditions for optimal stoichiometry are the same as those reported elsewhere.^{23,24} An atomic force microscope image of the sample, shown in Fig. 1(b), indicates that the VO₂ film consists of many individual grains with an in-plane size of about 100 nm. X-ray diffraction shows that the individual VO₂ grains are oriented such that the (011) plane of the monoclinic M₁ phase is in the plane of the substrate (See Fig. 1(c) and Ref. 21). This becomes the (110) plane in the rutile structure²¹. However, there is no preferred orientation of the grains with respect to rotations about the out of plane direction.

The first-order phase transition in this film exhibits the classic hysteresis usually observed in VO₂. The temperature dependent transmission through the VO₂ film-substrate system at 0.5 eV provides a clear picture of the hysteresis loop for the MIT in this particular film (See Fig. 1(d)). The photon energy of 0.5 eV is just below that of the energy gap in insulating VO₂ resulting in minimal absorption and high transmission intensity. The transmission drops with the occurrence of metallicity in the vicinity of the MIT due to the increased reflectance and absorption of the metallic phase. The T_c of the film is depressed from the bulk T_c of 340K to 325K. The 15K width of the hysteresis loop in this film is somewhat broader than what is seen in VO₂ crystals.²⁵ Such broadening of the hysteresis and the phase transition is typical of polycrystalline VO₂ thin films because of variation in grain size and strain inhomogeneity. This inhomogeneity is consistent with the width of the X-ray diffraction peak shown in Fig. 1(c).

B. Spectroscopic Methods

Spectroscopic measurements were performed to study the optical properties of the VO₂ film on quartz between 7.5 meV and 6.0 eV. This broad spectral range is necessary to characterize both the electronic and lattice degrees of freedom. Specifically, temperature dependent spectroscopic ellipsometry was performed in the spectral range between 0.6 eV and 6.0 eV at temperatures of 300K and 360K. The VO₂ is in the M₁ insulating phase at 300 K and in

the rutile metallic phase at 360 K. Due to its self-referencing nature, spectroscopic ellipsometry enables very precise measurement of the complex dielectric function of the sample. To extend our spectral range into the far-infrared, near-normal incidence reflectance between 7.5 meV and 1 eV was obtained at 300 K and 360 K. In addition to the VO₂ film on quartz, the same temperature dependent spectroscopic measurements were performed on the (001) quartz substrate. In order to obtain the optical constants of the VO₂ film, the ellipsometry and reflectance data for the substrate and the VO₂ film-substrate system was fit with Kramers-Kronig consistent Drude, Lorentzian, Tauc-Lorentzian, and Gaussian oscillators. We report the optical constants of the VO₂ film at 300K and 360K in the insulating and metallic phases respectively. Spectra and fits, in addition to technical details about the modeling procedure, are included in the Supplemental Material.²¹

III. RESULTS AND DISCUSSION

A. Sample Strain

In a polycrystalline thin film which is not lattice matched to the substrate, such as the one studied in this work, the resultant strain state of the film is particularly dependent on the growth technique. There are stresses which occur between neighboring grains, and have been shown to affect the T_c of VO₂.²⁶ Such strain is sensitive to the grain size and film microstructure and both these properties are influenced by the growth conditions. There are additional factors present in sputtered films²⁷. Of particular note is a process referred to as “shot peening”, in which compressive strain arises as a result of the sample being bombarded by energetic particles during growth. Compressive in-plane strain in sputtered oxide films is often attributed to this effect^{28,29}. Thermal strain from the mismatch of the coefficient of thermal expansion between the film and substrate may also be present.

The out of plane strain can be calculated by comparing the measured x-ray diffraction data shown in Fig. 1(c) with the literature. X-ray diffraction shows that the (011)_{M1} plane spacing is 3.23Å in the present sample. From the literature, the (011)_{M1} plane spacing ranges from 3.1978 Å and 3.2067 Å for bulk VO₂.^{30,31} Averaging the literature values implies a tensile strain in the out of plane direction of 0.89%. This type of tensile strain would result from compressive strains in the plane of the substrate. The transition temperature for the MIT is expected to be most sensitive to strain along the a_m (c_r) direction.³² Depression of T_c to 325K, as is the case in the our film, has been seen in VO₂ nanorods with a compressive strain of 1.5% along a_M .¹⁰ Similar strong dependence of the T_c as a function of strain has been seen in VO₂ films on TiO₂.³³ In both cases, compressive strain along a_m results in depression of the transition temperature. Thus it is reasonable to conclude that the VO₂ film studied in our work has a compressive strain of about 1.5% along a_M .

The a_M axis contracts by about 1% across the phase transition into the rutile phase. This would tend to relax compressive strains along c_r (a_m) in the metallic phase. Some partial

relaxation of the in-plane strain is evidenced by the shift of the x-ray diffraction peak towards the bulk rutile value shown in the Supplemental Material²¹. However, as the out of plane strain in the metallic phase is still tensile, the in plane strain is still somewhat compressive. Additional changes to the strain as the sample is heated across the MIT could be induced due to the mismatch of thermal expansion coefficients between the VO₂ film and quartz substrate. The coefficients of thermal expansion of a_r VO₂, c_r VO₂, and a-axis quartz are $4 \times 10^{-6}/K$, $25 \times 10^{-6}/K$, and $16 \times 10^{-6}/K$, respectively^{34,35}. Thus, this is at most a 0.1% effect over the 60K temperature range investigated in this work and has negligible impact on the strain state of the film.

Here we discuss the stoichiometry of the VO₂ films we have studied in this work. One effect of oxygen deficiency is to reduce T_c . However, oxygen deficiency also increases disorder in the film which significantly reduces the jump in the dc conductivity across the metal-insulator transition²³. In the films studied in our work, the optical conductivity in the low frequency limit changes by four orders of magnitude across the metal-insulator transition. This is consistent with stoichiometric VO₂ with minimal oxygen deficiency, comparable to single crystals. Moreover, the fact that we clearly see VO₂ optical phonon features in the spectra is further evidence that the film is composed of crystallites with minimal disorder due to oxygen deficiency. Hence the reduction in T_c in our films is due to compressive in-plane strain rather than oxygen deficiency.

B. IR active phonons and lattice dynamics

Due to the polycrystalline nature of the film, we measured the reflectance with unpolarized light. Thus, features due to infrared active phonons of both A_u and B_u symmetries are expected to appear in the reflectance data in the insulating M₁ phase. However, the relative strengths of each phonon will depend on the orientation of the dipole moment relative to the plane of the sample: phonons with in-plane dipole moments will have a larger contribution to the effective optical constants.^{19,20} The dipole moments of the A_u phonon modes, which lie parallel to b_M , are at 45 degrees out of the plane of the substrate in this film geometry. In contrast, the B_u modes have dipole moments in the a_M - c_M plane. Depending on the specific B_u mode in question, the dipole moments could be anywhere from 0 to 45 degrees out of plane. Thus, all 15 infrared active phonons should, in principle, contribute to the measured spectrum.

The measured imaginary part of the complex dielectric function in the phonon region is shown in Fig. 2(a). We are able to resolve 8 infrared-active phonons in this work. The infrared active phonons in VO₂ crystals have been previously characterized by optical spectroscopy.^{19,20} It is not unusual that we resolve fewer than the expected 15 infrared-active phonons, as some VO₂ phonons overlap. Moreover, the sample is a thin film, resulting in much weaker phonon features in comparison to those of the quartz substrate which dominate the measured spectrum in this region. More importantly, the clearly resolved VO₂ phonon center frequencies differ from the bulk values by at most 1.3% (See Fig. 2(b)). Raman spectroscopy performed on films grown by the same method also shows negligible shift in the phonon center frequencies

compared to bulk VO_2 .³⁶ Remarkably, the lattice dynamics are virtually unchanged relative to bulk VO_2 in a film where the T_c is so significantly depressed.

Previous experiments have seen that spectral features due to the rutile phase phonons are fairly weak and difficult to resolve from the metallic background.^{19,20} In this work, IR active phonon features in the rutile phase are not observed in the reflectance spectrum. Apart from the high conductivity of VO_2 in the metallic phase, the absence of rutile phonon features in this work can be attributed to the thin film nature of the sample and strong phonon features of the quartz substrate.

C. Inter-band transitions and electronic structure

1. Assignment of spectral features

In the absence of polarization dependent data, features in the optical conductivity cannot be unambiguously assigned to specific interband transitions. However, energy scales of the measured spectral features can still be discussed within the context of band theoretical results on VO_2 .^{37,38} A schematic view of the band structure of VO_2 is shown in Fig. 3 to support the following discussion. Note that the lower and upper Hubbard bands, which, in the rutile phase, arise from electronic correlations not considered by conventional band theory, are shown explicitly in Fig. 3.

The measured optical conductivity for the rutile phase at 360K is shown in Fig. 4(a). Some of the lower energy inter-band transitions in this compressively strained sample differ significantly from those measured previously on bulk VO_2 and thin films.^{12–14,19} The VO_2 film on quartz exhibits a broad Drude-like metallic response “q” and an interband transition “s” which are consistent with previous works. Feature “s” at 3.1 eV is attributed to transitions between the O_{2p} orbitals and the vanadium e_g^π bands. However, in this strained VO_2 film on quartz, we resolve additional features: a pseudo-gap type feature in the low frequency electronic response “p”, and well-defined features, “r” and “t”, at 2.2 and 5eV, respectively. The pseudo-gap type feature, “p”, has been seen in a few previous works.^{20,39} Compressive strain along c_r is expected to lower the energy of the a_{1g} band¹¹. That compressive strain results in a lowering of the energy of the a_{1g} band is supported by X-ray emission spectroscopy experiments on strained VO_2 films grown on TiO_2 .⁴⁰ The slight lowering of the filled a_{1g} bands relative to the e_g^π bands could account for the prominence of the pseudo-gap type feature “p” if this feature is due to optical transitions between those two bands. This lowering in energy of the a_{1g} band, due to compressive strain, would increase the occupation of the bottom half of the a_{1g} band. Increased occupation of the a_{1g} band could lead to a reduction in screening and an increase in electronic correlation effects for electrons in the a_{1g} bands, similar to the explanation presented by Zylbersztein and Mott for the insulating M_1 phase.¹⁵

Correlation effects in the rutile phase could lead to a degree of splitting of the a_{1g} band into lower and upper Hubbard bands.⁴¹ A “satellite” of the a_{1g} band, consistent with this type of lower Hubbard band, has been seen previously in photoemission experiments on bulk VO₂.⁴² We interpret feature “r” as transitions from the filled parts of the a_{1g} bands (both the unsplit portion and the lower Hubbard band) to the unfilled upper Hubbard band. Such splitting could also account for feature “t” if it is assigned to the transition between the O_{2p} and upper Hubbard bands. There is also likely some absorption near 5 eV due to transitions between the O_{2p} and e_g^σ bands, as the O_{2p} to e_g^π transition is seen at 3 eV, and the crystal field splitting between e_g^π and e_g^σ is expected to be on the order of 2 eV.⁴³ That a well resolved feature at 5 eV is not present in the M₁ phase supports the assignment of feature “t” to a transition involving the upper Hubbard bands, as these bands might be expected to shift more significantly across the MIT. In this scenario, the upper Hubbard band would need to lie at an energy very close to that of the e_g^σ bands. This would imply a correlation induced Hubbard splitting of a comparable magnitude to the crystal field splitting, and is expected to be much larger than the splitting caused by a Peierl’s type lattice distortion.

Increased correlations due to compressive strain, as discussed above, would result in more states being shifted into the satellites of the a_{1g} orbital, and could account for why we are able to clearly resolve features “r” and “t” in this sample. It is also possible that correlation effects lead to significant splitting of the a_{1g} bands even in the unstrained rutile phase. Subtle evidence of a transition between the Hubbard bands was seen previously in rutile VO₂ on sapphire near 3 eV.¹³ However, this feature could not be clearly resolved from the O_{2p} to e_g^π transition. Thus, it’s also possible that this feature has in fact been shifted to a lower energy in our particular film.

The measured optical conductivity for the M₁ phase at 300K is shown in Fig. 4(a). Features “A” and “C” are consistent with previous works.^{12–14} Feature “A” is attributed to transitions between the filled bonding a_{1g} and the empty e_g^π bands, while feature “C” is attributed to transitions between the filled O_{2p} and empty e_g^π bands.

We observe an additional feature, “B”, which is different from previous works. While a strong feature at low energy, around 0.9 eV, is seen in single crystals for light perpendicular to a_M ,¹² feature B in the present work is somewhat stronger and at a much higher energy, 1.9eV. A similar strong feature at 1.9 eV is not seen in previous work on thin films grown on sapphire and TiO₂.^{13,14}

Interestingly, the transition between a_{1g} and a_{1g}^* , which has been seen in previous experiments on bulk crystals and thin films around 2.5eV,^{12,13} is not clearly present near this energy in the VO₂ on quartz data. It is likely that this transition has been down-shifted as a result of strain. It is possible that feature “B” is in fact the a_{1g} to a_{1g}^* transition, having been shifted to lower energies in this particular film. Such an interpretation is not unreasonable, given that the analogous feature in the rutile, feature “r”, occurs at a very similar energy to

feature “B”. However, recent DMFT calculations show that the splitting between a_{1g} and a_{1g}^* should increase with compressive strain along the a_M axis.³² Such an increase in splitting would result in a shift of the a_{1g} to a_{1g}^* transition to higher energies, into the vicinity of feature C. Indeed, there is fine structure in feature “C” that would be consistent with such an explanation.

Note that the evidence for Hubbard bands in the rutile metal suggests that correlation effects are significant enough to govern the evolution of VO₂ properties upon lowering temperature. In Goodenough’s band theory picture, the anti-ferroelectric displacement of the vanadium atoms in the M₁ structure is necessary to raise the energy of the e_g^π bands above the Fermi energy to produce an energy gap.¹¹ It is interesting to note, however, that in both the present experiment and previous work,¹³ the O_{2p} to e_g^π transition is not shifted appreciably, certainly much less than the 0.6eV band gap of M₁ VO₂. This could indicate that the e_g^π band itself is not as strongly dependent on the change in lattice symmetry as expected. Alternatively, the O_{2p} bands may also shift significantly across the phase transition.

2. Spectral weight transfer

As the “f-sum rule” is a fundamental statement of conservation of charge in a material, it should be conserved across the MIT. The total spectral weight (A_{total}) is conserved as follows. Note that the following equations employ Gaussian (cgs) units.

$$A_{total} \equiv \int_0^\infty \sigma_1(\omega) d\omega = \frac{n\pi e^2}{2m_0V} \quad (1)$$

Where $\sigma_1(\omega)$ is the real part of the optical conductivity as a function of photon energy $\hbar\omega$, n is the number of electrons in a volume V of the material, e is the elementary charge, and m_0 is the free electron mass. By integrating to a finite frequency, one can consider the spectral weight (A) below a certain photon energy ($\hbar\omega_c$).

$$A(\omega_c) = \int_0^{\omega_c} \sigma_1(\omega) d\omega \quad (2)$$

It is interesting to define N_{eff} which, in the spirit of equations (1) and (2), gives us the *effective* number of carriers with optical mass equal to m_0 that contribute to absorption below a certain photon energy, $\hbar\omega_c$.

$$N_{eff}(\omega_c) = \frac{2m_0V}{\pi e^2} \int_0^{\omega_c} \sigma_1(\omega) d\omega \quad (3)$$

The optical conductivity and effective number of carriers is shown in Fig. 4(b) as a function of photon energy. The volumes used for this calculation is $\frac{1}{2}$ of the rutile³⁴ and $\frac{1}{4}$ of the M_1 ³¹ unit cell volumes from the literature. This corresponds to the volume of a single formula unit, and thus a single vanadium atom. While there are some slight shifts in spectral weight up to and exceeding 6eV, 95% of the spectral weight has been recovered by 4 eV. That the f-sum rule is still not fully satisfied at such high energies clearly indicates a rearrangement of the electronic structure at even higher energies. For example, feature “t”, clearly resolved in the rutile phase at 5 eV, is not present in the M_1 phase. Such rearrangement at higher energy scales supports the hypothesis that the MIT in VO_2 is electronically driven. Previous optical spectroscopy measurements have also shown shifts in spectral weight across the MIT up to and exceeding 6 eV.^{13,14}

The spectral weight of the conduction electrons (features “q” and “p”) in the rutile phase will be largely contained below 1.8eV in the broad-Drude-like feature. While one might naively expect one conduction electron per vanadium atom, N_{eff} at this energy is only 0.21. This indicates that either the effective electron mass (m^*) of the conduction electrons is several times m_0 and/or the spectral weight of the correlated vanadium 3d electrons has shifted to energies higher than 1.8 eV.

IV. CONCLUSIONS

The properties of strongly correlated condensed matter systems can change dramatically when subject to external perturbations such as strain. In the VO_2 film on quartz film investigated in this work, compressive strain along the a_M (c_r) direction results in the T_c being shifted down to 325K from the bulk T_c of 340K. Broadband infrared and optical spectroscopy was used to characterize both the electronic and lattice-structural degrees of freedom in this film to elucidate the cause of this significant change in T_c , and its implications regarding the nature of the MIT in VO_2 .

Strain affects the inter-band transitions by altering the relative energies of the bands, as well as their orientation in real space. Such changes can have important implications in correlated system where the Coulomb repulsion between electrons, orbital overlaps, and screening play nontrivial roles. Indeed, some of the inter-band transitions in this strained VO_2 film differ significantly from those measured previously in bulk crystals and thin films. In particular, two new features are observed. Features at 2.2 eV and 5.2 eV are observed in the rutile phase which we attribute to transitions between the filled a_{1g} and O_{2p} states and the upper Hubbard band. It is possible that this feature is more prominent because the compressive strain along c_r increases the occupation of the a_{1g} orbital, thereby reducing screening and enhancing correlation effects. A new feature is seen around 1.9eV in the monoclinic M_1 phase; the values of ϵ_2 and σ_1 are significantly higher at this energy than in bulk crystals or other thin films. A definitive assignment of the a_{1g} to a_{1g}^* optical inter-band

transition is not possible at present although there are two possible scenarios: Either it has been shifted down to 1.9 eV due to strain and appears as feature “B”, or it appears as fine structure in feature “C” near 3 eV.

Interestingly, unlike the inter-band transitions, the infrared active phonons in these strained films are very similar to their bulk counter-parts, indicating that the forces between the vanadium and oxygen ions remain largely unchanged despite the strained nature of this film. Nevertheless, this strain is sufficient to cause significant changes in the transition temperature and the optical inter-band transitions. This would indicate that the T_c is more sensitive to changes in the orbital overlaps and occupation than it is to changes in the lattice dynamics. It is reasonable to conclude that the MIT in VO_2 is more likely to be driven by changes in electronic correlations and orbital occupations rather than by lattice dynamics. The change in lattice structure could then occur as a consequence of the variations in electronic structure and interactions.

As the electronic and optical properties of VO_2 are incredibly sensitive to strain, this system has potential for applications as strain engineering could be used to tune these properties. We have measured and documented the infrared and optical properties of VO_2 film on quartz substrate. This is a necessary step towards fully realizing the potential of strain engineering this material.

ACKNOWLEDGEMENTS

MMQ is grateful for financial support from NSF DMR (grant # 1255156) and the Jeffress Memorial Trust. RAL, SW and JL also acknowledge support from the NRI/SRC sponsored ViNC center and the Commonwealth of Virginia through the Virginia Micro-Electronics Consortium (VMEC).

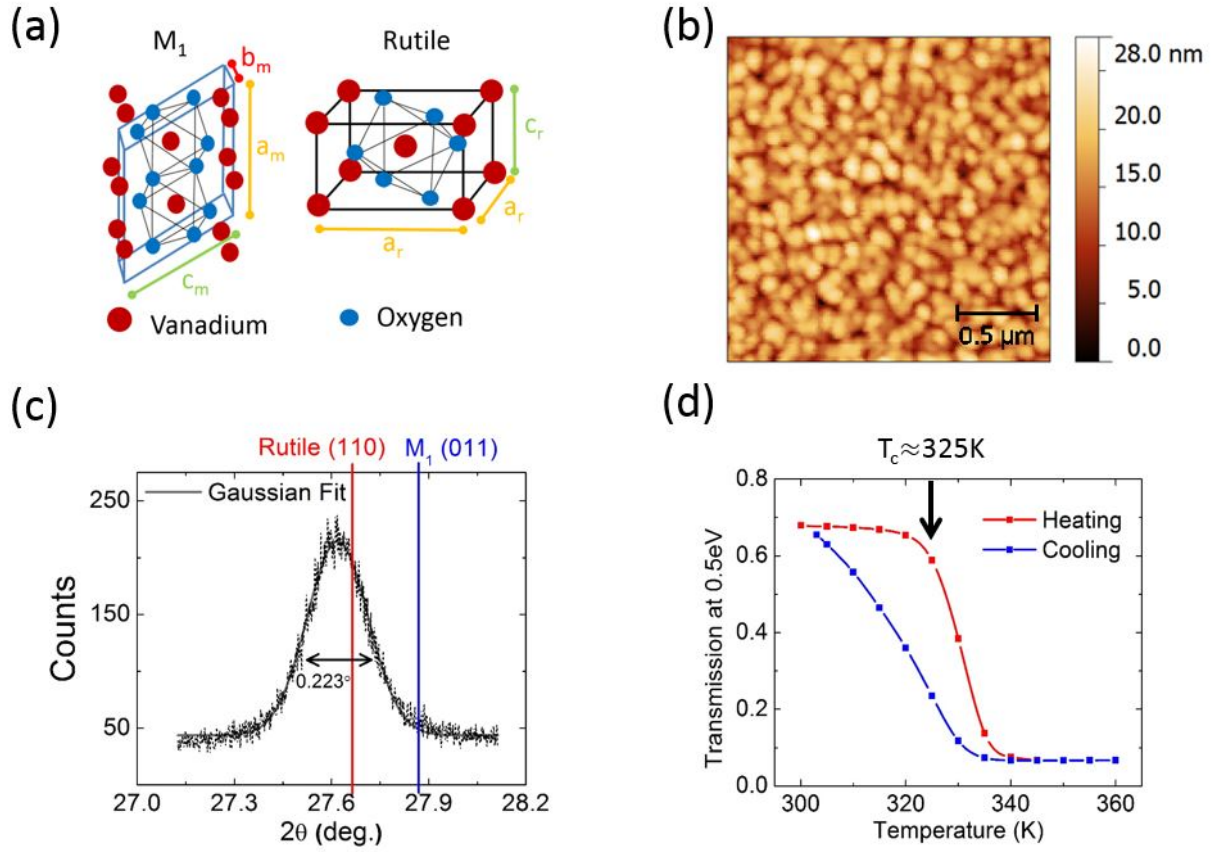


FIG. 1. Color online (a) Lattice structure of the M_1 and Rutile phases of VO_2 . (b) AFM image at room temperature showing the surface roughness and multi-grain structure of the $(011)_{M_1}$ VO_2 film on quartz substrate. (c) X-ray diffraction peak resulting from the $(011)_{M_1}$ lattice planes. The Gaussian fit and resulting full width at half maximum is shown. The peak positions for the bulk $(011)_{M_1}$ and analogous (110) rutile diffraction spots are shown as vertical lines. (d) Transmission through the sample at a photon energy of 0.5 eV, demonstrating the temperature dependence of the transition during heating and cooling runs. Note the T_c onset of 325K is significantly lower than that of bulk crystals (340K).

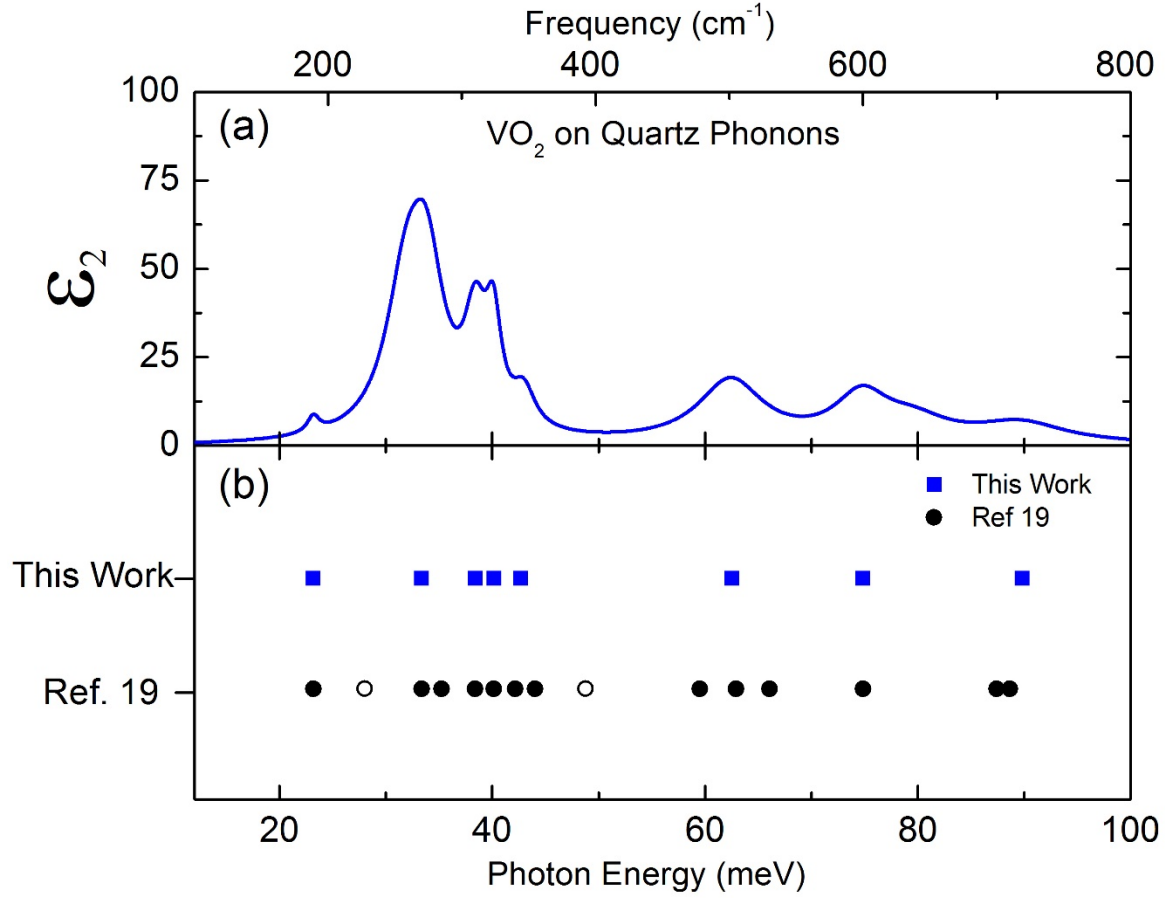


FIG. 2. Color online (a) Measured imaginary part of the complex dielectric function (ϵ_2) in the phonon region. (b) The measured center frequencies of the IR active phonons are compared to previous data taken on bulk crystals¹⁹. Open circles denote phonon modes from Ref. 19 that are not obvious in the spectra measured in this work (See Text).

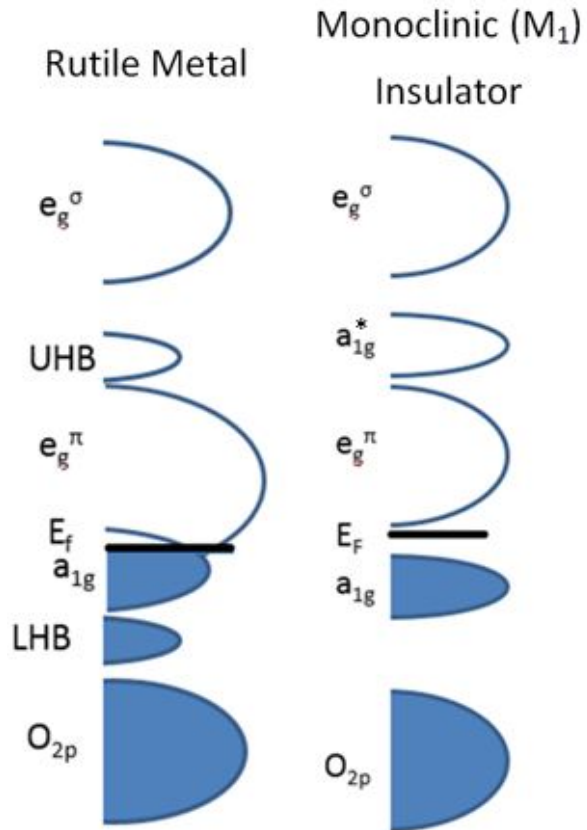


FIG. 3. Schematic showing energy levels of the relevant vanadium and oxygen bands in the metallic and insulating states of VO_2 . The Fermi level is denoted as E_F . The possible (partial) Hubbard splitting of the a_{1g} band due to correlation effects in the rutile metal is shown explicitly.

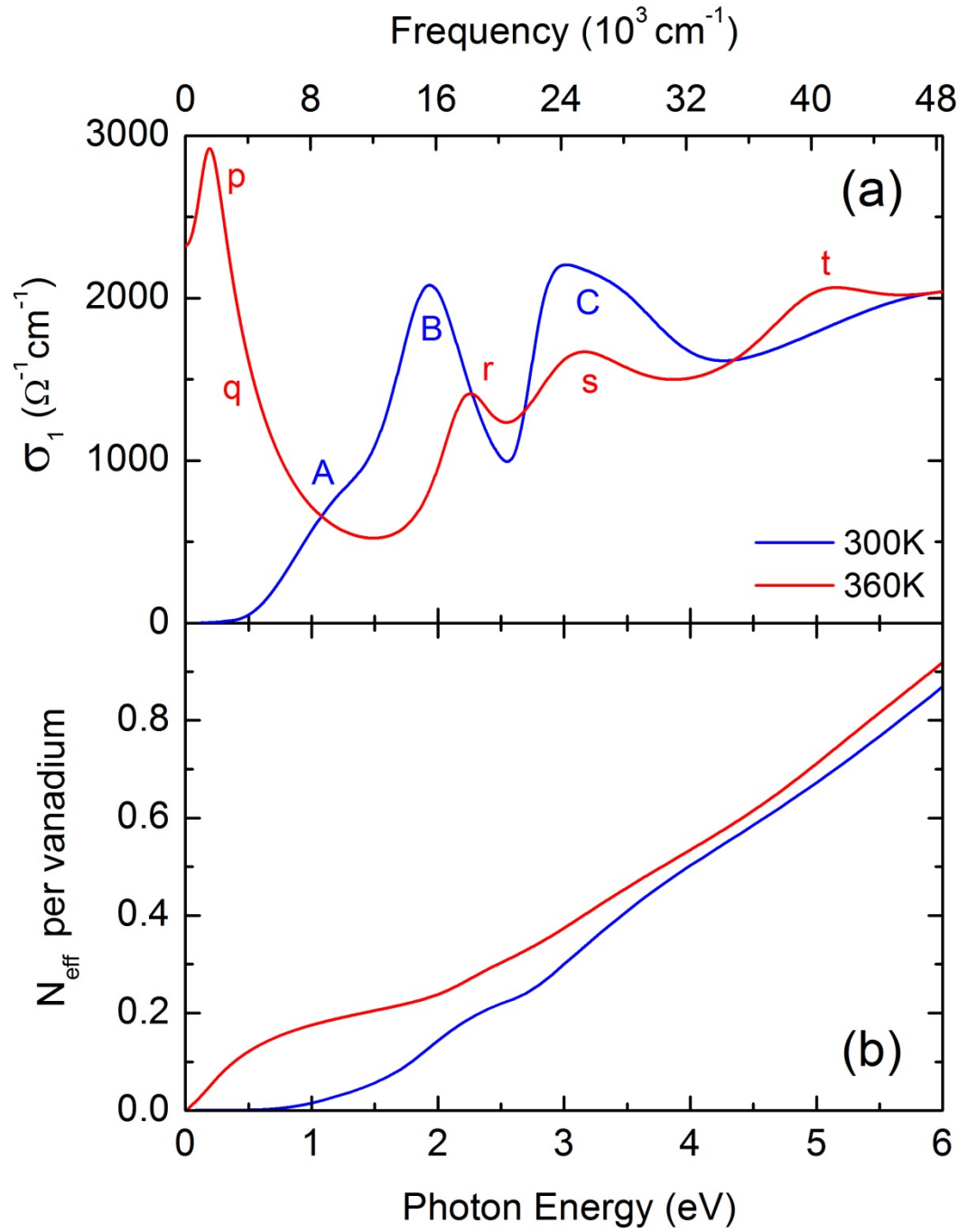


FIG. 4. Color online (a) Optical conductivity σ_1 for the rutile (red) and M_1 (blue) phases as a function of photon energy. Phonons have been subtracted from the conductivity of the M_1 phase. Spectral features are denoted by lower and upper case letters for the rutile and M_1 phases respectively. The assignment of these spectral features to specific inter-band transitions is discussed in the text. (b) The effective number of carriers per vanadium atom (See text).

* Correspondence should be addressed to MMQ at mumtaz@wm.edu

¹ M. Imada, A. Fujimori, and Y. Tokura, Reviews of Modern Physics **70**, 1039 (1998).

² D.C. Johnston, Advances in Physics **59**, 803 (2010).

³ D.N. Basov, R.D. Averitt, D. van der Marel, M. Dressel, and K. Haule, Reviews of Modern Physics **83**, 471 (2011).

⁴ E. Dagotto, Science **309**, 257 (2005).

⁵ E. Arcangeletti, L. Baldassarre, D. Di Castro, S. Lupi, L. Malavasi, C. Marini, A. Perucchi, and P. Postorino, Physical Review Letters **98**, 196406 (2007).

⁶ C. Marini, E. Arcangeletti, D. Di Castro, L. Baldassarre, a. Perucchi, S. Lupi, L. Malavasi, L. Boeri, E. Pomjakushina, K. Conder, and P. Postorino, Physical Review B **77**, 235111 (2008).

⁷ J.M. Atkin, S. Berweger, E.K. Chavez, M.B. Raschke, J. Cao, W. Fan, and J. Wu, Physical Review B **85**, 020101 (2012).

⁸ N.B. Aetukuri, A.X. Gray, M. Drouard, M. Cossale, L. Gao, A.H. Reid, R. Kukreja, H. Ohldag, C. a. Jenkins, E. Arenholz, K.P. Roche, H. a. Dürr, M.G. Samant, and S.S.P. Parkin, Nature Physics **9**, 661 (2013).

⁹ J.H. Park, J.M. Coy, T.S. Kasirga, C. Huang, Z. Fei, S. Hunter, and D.H. Cobden, Nature **500**, 431 (2013).

¹⁰ J. Cao, Y. Gu, W. Fan, L.Q. Chen, D.F. Ogletree, K. Chen, N. Tamura, M. Kunz, C. Barrett, J. Seidel, and J. Wu, Nano Letters **10**, 2667 (2010).

¹¹ J.B. Goodenough, J.Solid State Chem. **3**, 490 (1971).

¹² H.W. Verleur, A.S. Barker, and C.N. Berglund, Physical Review **172**, 788 (1968).

¹³ M.M. Qazilbash, A.A. Schafgans, K.S. Burch, S.J. Yun, B.G. Chae, B.J. Kim, H.T. Kim, and D.N. Basov, Physical Review B **77**, 115121 (2008).

¹⁴ K. Okazaki, S. Sugai, Y. Muraoka, and Z. Hiroi, Physical Review B **73**, 165116 (2006).

¹⁵ A. Zylbersztejn, N.F. Mott, and A.Z. and N.F. Mott, Physical Review B **11**, 4383 (1975).

¹⁶ D. Paquet and P. Lerouxhugon, Physical Review B **22**, 5284 (1980).

¹⁷ T.M. Rice, H. Launois, and J.P. Pouget, Physical Review Letters **73**, 3042 (1994).

¹⁸ J.P. Pouget, H. Launois, J.P. Dhaenens, P. Merenda, and T.M. Rice, Physical Review Letters **35**, 873 (1975).

- ¹⁹ A.S. Barker, H.W. Verleur, and H.J. Guggenheim, *Physical Review Letters* **17**, 1286 (1966).
- ²⁰ T.J. Huffman, P. Xu, M.M. Qazilbash, E.J. Walter, H. Krakauer, J. Wei, D.H. Cobden, H.A. Bechtel, M.C. Martin, G.L. Carr, and D.N. Basov, *Physical Review B* **87**, 115121 (2013).
- ²¹ See Supplemental Material at [URL Inserted by Publisher] for Technical Details of the Data Analysis and Tabulated Optical Constants. (n.d.).
- ²² K.G. West, J. Lu, J. Yu, D. Kirkwood, W. Chen, Y. Pei, J. Claassen, and S.A. Wolf, *Journal of Vacuum Science and Technology A: Vacuum, Surfaces, and Films* **26**, 133 (2008).
- ²³ S. Kittiwatanakul, J. Laverock, D. Newby, K.E. Smith, S. a. Wolf, and J. Lu, *Journal of Applied Physics* **114**, 053703 (2013).
- ²⁴ K.G. West, J. Lu, J. Yu, D. Kirkwood, W. Chen, Y. Pei, J. Claassen, and S. a. Wolf, *Journal of Vacuum Science & Technology A: Vacuum, Surfaces, and Films* **26**, 133 (2008).
- ²⁵ B.S. Mun, K. Chen, J. Yoon, C. Dejoie, N. Tamura, M. Kunz, Z. Liu, M.E. Grass, S.-K. Mo, C. Park, Y.Y. Lee, and H. Ju, *Physical Review B* **84**, 113109 (2011).
- ²⁶ R.A. Aliev, V.N. Andreev, V.M. Kapralova, V.A. Klimov, A.I. Sobolev, and E.B. Shadrin, *Physics of the Solid State* **48**, 929 (2006).
- ²⁷ H. Windischmann, *Critical Reviews in Solid State and Materials Sciences* **17**, 547 (1992).
- ²⁸ W.Y. Park, K.H. Ahn, and C.S. Hwang, *Applied Physics Letters* **83**, 4387 (2003).
- ²⁹ T. Ashida, K. Kato, H. Omoto, and A. Takamatsu, *Japanese Journal of Applied Physics* **49**, 065501 (2010).
- ³⁰ G. Andersson, *Acta Chemica Scandinavica* **10**, 623 (1956).
- ³¹ J.M. Longo and P. Kierkega, *Acta Chemica Scandinavica* **24**, 420 (1970).
- ³² B. Lazarovits, K. Kim, K. Haule, and G. Kotliar, *Physical Review B* **81**, 115117 (2010).
- ³³ Y. Muraoka, Y. Ueda, and Z. Hiroi, **63**, 965 (2002).
- ³⁴ D.B. Mcwhan, M. Marezio, J.P. Remeika, and P.D. Dernier, *Physical Review B* **10**, 490 (1974).
- ³⁵ A.H. Jay, *Proceedings of the Royal Society of London* **142**, 237 (1933).
- ³⁶ E. Radue, E. Crisman, L. Wang, S. Kittiwatanakul, J. Lu, S. a. Wolf, R. Wincheski, R. a. Lukaszew, and I. Novikova, *Journal of Applied Physics* **113**, 233104 (2013).
- ³⁷ V. Eyert, *Ann.Phys.(Leipzig)* **11**, 650 (2002).

- ³⁸ S. Biermann, A. Poteryaev, A.I. Lichtenstein, and A. Georges, Physical Review Letters **94**, 26404 (2005).
- ³⁹ M.M. Qazilbash, M. Brehm, B.-G. Chae, P.-C. Ho, G.O. Andreev, B.-J. Kim, S.J. Yun, A. V Balatsky, M.B. Maple, F. Keilmann, H.-T. Kim, and D.N. Basov, Science **318**, 1750 (2007).
- ⁴⁰ J. Laverock, L.F.J. Piper, a. R.H. Preston, B. Chen, J. McNulty, K.E. Smith, S. Kittiwatanakul, J.W. Lu, S. a. Wolf, P. -a. Glans, and J.-H. Guo, Physical Review B **85**, 081104 (2012).
- ⁴¹ S. Biermann, A. Georges, A. Lichtenstein, and T. Giamarchi, Physical Review Letters **87**, 276405 (2001).
- ⁴² T.C. Koethe, Z. Hu, M.W. Haverkort, C. Schuessler-Langeheine, F. Venturini, N.B. Brookes, O. Tjernberg, W. Reichelt, H.H. Hsieh, H.-J. Lin, C.T. Chen, and L.H. Tjeng, Physical Review Letters **97**, 116402 (2006).
- ⁴³ C. Sommers, R. de Groot, D. Kaplan, and A. Zylbersztejn, Journal De Physique Lettres **36**, L157 (1975).

